

<https://helda.helsinki.fi>

Revealing microbial processes and nutrient limitation in soil
through ecoenzymatic stoichiometry and glomalin-related soil
proteins in a retreating glacier forefield

Jiang, Yonglei

2019-03-15

Jiang , Y , Lei , Y , Qin , W , Korpelainen , H & Li , C 2019 , ' Revealing microbial processes and nutrient limitation in soil through ecoenzymatic stoichiometry and glomalin-related soil proteins in a retreating glacier forefield ' , *Geoderma* , vol. 338 , pp. 313-324 . <https://doi.org/10.1016/j.geoderma.2018.12.023>

<http://hdl.handle.net/10138/323509>

<https://doi.org/10.1016/j.geoderma.2018.12.023>

cc_by_nc_nd

acceptedVersion

Downloaded from Helda, University of Helsinki institutional repository.

This is an electronic reprint of the original article.

This reprint may differ from the original in pagination and typographic detail.

Please cite the original version.

**Revealing microbial processes and nutrient limitation in soil through coenzymatic stoichiometry
and glomalin-related soil proteins in a retreating glacier forefield**

Yonglei Jiang ^a, Yanbao Lei ^b, Wei Qin ^c,

Helena Korpelainen ^d and Chunyang Li ^{a, *}

^a College of Life and Environmental Sciences, Hangzhou Normal University, Hangzhou 310036, China

^b Key Laboratory of Mountain Surface Processes and Ecological Regulation, Institute of Mountain Hazards
and Environment, Chinese Academy of Sciences, Chengdu 610041, China

^c Department of Soil Quality, Wageningen University and Research, P.O. Box 47, 6700 AA Wageningen,
The Netherlands

^d Department of Agricultural Sciences, Viikki Plant Science Centre, University of Helsinki, P.O. Box 27,
FI-00014, Finland

* Correspondence author: e-mail: licy@hznu.edu.cn

Abstract

The glacial retreat is observed and predicted to increase in intensity especially in high-elevation areas as a result of global warming, which leaves behind a primary succession along soil chronosequences. Although soil microbes have been recognized as main drivers of ecological and evolutionary processes, our understanding of their effects on nutrient biogeochemistry during primary succession remains limited. In this study, we investigated changes in the microbial community structure, coenzymatic stoichiometry, and glomalin-related soil protein (GRSP) accumulation in the *Hailuogou Glacier Chronosequence*, located on the eastern Tibetan Plateau. We wanted to reveal the effects of nutrient limitation on soil microbes and the relative contributions of edaphic and biotic factors. The results showed that with an increasing soil age, there was a steady increase in the microbial biomass and a shift from a bacterial to fungal dominated pattern. Soil enzyme stoichiometry and analyses on threshold elemental ratios revealed that microbial activities are limited by carbon and nitrogen during the early successional stage (3-52 years), while phosphorus was the main limiting factor during later stages (80-120 years). Moreover, the redundancy analysis and structural equation modeling suggested that during early stages edaphic factors had a greater impact on microbial processes, while the vegetation factors were most influential during the last two stages. Overall, these results highlighted the importance of integrating knowledge of the microbial community structure, soil enzyme activities and GRSP to gain a holistic view of soil-plant-microbe interactions during ecosystem successions.

Key words Soil extracellular enzymes; Glomalin-related soil protein; Bacterial and fungal community structure; *Hailuogou Glacier Chronosequence*.

1. Introduction

Global warming has accelerated the retreat of glaciers, which has resulted in the development of new terrains containing mineral debris for the colonization by terrestrial microorganisms and pioneer plants (Schmidt et al., 2016). The glacial retreat areas provide an excellent opportunity to study the succession of plant and microbial communities, and also their interactions that contribute to soil ecosystem functioning (Knelman et al., 2012; Insam et al., 2017). Soil microorganisms are strongly involved in the plant community succession, soil nutrient release and retention. Many studies have shown that the composition and activity of soil microbial communities exhibit distinct patterns at different succession stages along the retreat of glaciers (Knelman et al., 2012; Schmidt et al., 2016; Insam et al., 2017; Jiang et al., 2018). For example, previous studies conducted on the High Arctic glacier foreland have shown that the microbial respiration rate and biomass are generally low at the early stages of succession and tend to increase with the progress of succession (Yoshitake et al., 2007; 2018). Furthermore, Sørensen et al. (2006) found that the addition of both carbon and nutrient (nitrogen and phosphorus) engendered a higher respiration rate and higher densities of soil fauna in dry heath (snowmelt occurs earlier) compared to the mesic heath (snowmelt occurs later) soils at a High Arctic site. Thus, soil microorganisms together with nutrient dynamics can be used to predict soil-plant-microbe interactions and soil biogeochemical cycles during ecosystem successions.

Soil extracellular enzymes produced by plants and microorganisms decompose organic matter present in soil. The expression of enzymes is a product of cellular metabolism, particularly regulated by the availability of nutrients in their environment (Sinsabaugh et al., 2009). The relative abundance of enzymes involved in C, N and P cycling, namely extracellular enzyme stoichiometry, reflects the biogeochemical equilibrium between the metabolic and nutrient requirements of microbial assemblages and nutrient availability

(Sinsabaugh et al., 2009; Hill et al., 2012). Recently, coenzymatic stoichiometry has been suggested as a useful indicator of the relative resource limitation of microbial assemblages and their environment, because extracellular enzyme activities reflect the response of a microbial cell to meet its metabolic resource demands (Sinsabaugh et al., 2009; Chen et al., 2018).

Most early case studies and meta-analyses have indicated that there is a 1:1:1 converging tendency in C:N:P ratios of microbial acquisition activities (Sinsabaugh et al., 2008) and that the occurrence of C limitation is widespread among microbes. However, recent studies have suggested that N and P limitation are also common (Camenzind et al., 2017). For example, based on a meta-analysis of microbial enzyme activities in tropical ecosystems, Waring et al. (2013) found that nutrient cycling is more P-limited, as reflected by lower enzymatic N:P and C:P ratios. In contrast to the expected 1:1:1 ratio, Peng and Wang (2016) found that the ratio of C-, N- and P-acquiring enzyme activities is 1:1.2:1.4 in the temperate grasslands of northern China. Furthermore, Peng and Wang (2016) found a higher microbial enzyme N:P ratio (0.38) in the temperate grasslands compared to tropical ecosystems (0.13) (Waring et al., 2013), which suggested that N is a limiting element, and microbes exhibit a stronger capacity to acquire N than P in temperate grasslands. According to Sinsabaugh et al. (2009; 2011), eco-enzyme activities are related to both the Ecological Stoichiometry Theory (EST) and the Metabolic Theory of Ecology (MTE), which can be illuminated via the Threshold Elemental Ratio (TER), when growth responds to nutrient limitation (represented by N and P, high C:N or C:P) and energy availability (represented by C, lower C:N or C:P). During a long-term ecosystem development, both the mineral composition and nutrient content of soil change, thus possibly altering microbial nutrient cycling by constraining substrate accessibility (Chen et al., 2018). For example, Yoshitake et al. (2007) found that microbial activity was limited by the low availability of both carbon and nitrogen at the early stage of succession, and nitrogen limitation is mitigated at the late stage of succession through the

addition of carbon and/or nitrogen. However, no significant changes were observed in the microbial biomass during succession. These findings are related to changes in the physiological activities of the microbial community, such as enzymatic activity. Thus, a more detailed quantitative characterization of soil enzyme stoichiometry and resource limitation during the primary succession is urgently needed to understand the responses of soil microbes. Such knowledge would help to elucidate the processes that affect soil fertility and to predict the responses of ecosystems to global change.

Microbial communities have a role in the soil development also through the maintenance of the soil structure, retention of nutrients and improvement of nutrient availabilities (Smith and Read, 2008). One of the most important N-linked glycoproteins secreted by arbuscular mycorrhizal fungi (AMF) is the glomalin-related soil protein (GRSP), which generally contains 3–5% N, 36–59% C, 0.03–0.1% P, and 2–5% Fe (Lovelock et al., 2004; Schindler et al., 2007; Singh et al., 2013). Sinsabaugh et al. (2009) have found that compared to the microbial biomass, GRSP contributes over 20 times more to soil organic carbon. Moreover, due to its hydrophobic, iron binding and ‘sticky-string-bag’ structure formed by the hyphae, GRSP reduces organic carbon turnover and enhances its sequestration in terrestrial ecosystems (Rillig, 2004; Smith and Read, 2008). Therefore, GRSP concentrations are considered as a sensitive indicator of soil quality (Zhang et al., 2017). A number of studies have linked GRSP to long-term C and N storage (Rillig et al., 2003; Lovelock et al., 2004). For example, Zhang et al. (2017) observed that the contribution of GRSP to SOC was 4.7% in the planted forest, which was 2.1 and 1.6 times greater than those in the secondary and primary forest, respectively. However, little data are available on the interaction between GRSP and soil microbial C-, N- and P-cycling enzymes, as well as on different contributions of GRSP to soil carbon pools at various stages of soil development in glacial retreat areas.

116 The *Hailuogou Glacier Chronosequence* in Southwestern China represents a primary succession
117 chronosequence and consists of different vegetation succession stages from pioneer communities to climax
118 vegetation communities (Yang et al., 2014; Lei et al., 2015; Wang et al., 2016). Along with the soil
119 development and plant community establishment, soil organic material and litter quality intensify plant–soil
120 interactions in these pristine environments. Precise knowledge of such interactions is crucial for
121 understanding the direction and magnitude of ecosystem succession (Wang et al., 2016; Jiang et al., 2018).
122 To address nutrient cycling processes during the primary ecosystem succession, we quantified microbial
123 abundance and community structures, activities of C- (BG and CBH), N- (NAG LAP) and P- acquiring (AP)
124 and organic matter degrading (POX) enzymes, as well as the potential substrate availability and the
125 physicochemical and mineral controls in the soil along the 120 year-old *Hailuogou Glacier Chronosequence*.
126 Our main objectives were to reveal the successional trajectories of microbial communities, as well as their
127 impact on glomalin-related soil protein accumulation and extracellular enzyme stoichiometry, and to
128 identify the limiting nutrient and relative contributions from edaphic and biotic factors in a retreating glacier
129 forefield. Specifically, we hypothesized that (1) along the successional stages, a more fungus-dominated
130 microbial structure elicits higher GRSP contributions that would improve the soil substrate quality (e.g., soil
131 organic C and total N contents); (2) the extracellular enzyme stoichiometry reflects soil nutritional status,
132 and the nutrient limiting factor shifts from C and N at early stages to N and P during later stages; (3) the
133 relative contributions of edaphic and biotic factors on microbial nutrient (C, N and P) cycling through soil
134 eco-enzyme stoichiometry and GRSP accumulation depend on the successional stage. By integrating the
135 microbial community structures, soil enzyme activities and GRSP into a holistic ecosystem nutrition model,
136 our results will provide new knowledge of the control of soil fertility along the successional stages in the
137 *Hailuogou Glacier Chronosequence*, as well as of the direction and magnitude of its responses to global
138 changes.

2. Materials and methods

2.1. Study sites

The Hailuoguo Glacier is a monsoonal temperate glacier located at the Gongga Mountain (29°30' to 30°20'N, 101°30' to 102°15'E, 7556 m a.s.l) on the south-eastern fringe of the Tibetan Plateau. Many types of scientific investigations have been conducted in the area, including research on hydrology, botany, soil carbon dynamics and microbiology (Lei et al., 2015; Wang et al., 2016), and thus detailed information about the *Hailuoguo Glacier Chronosequence* is available. The chronosequence extends to the northeast and has a horizontal length of 2 km and an elevation difference of 100 m. In this area, the climate is characterized by a mean annual precipitation of 2000 mm, most rainfall occurring between June and October (Lei et al., 2015), and considerable seasonal temperature fluctuations, ranging from -4.3 °C in January to 11.9 °C in July, with an annual mean temperature of 3.8 °C. The present study was conducted on seven sites (representing successional ages 3, 12, 30, 40, 52, 80 and 120 years) undergoing long-term primary succession from bare soil with low carbon and nitrogen, to pioneer communities and eventually to climax vegetation communities (Lei et al., 2015). Based on a survey, we found that *Astragalus* spp. is the dominant species at the 3-year stage, *Hippophae rhamnoides* L. and *Salix magnifica* are the dominant species at the 12-year stage, *H. rhamnoides*, *Salix* spp. and *Populus purdomii* are the dominant species at the 30- to 40-year stages, *Betula utilis*, *P. purdomii*, *Abies fabri* are the dominant species at the 52-year stage, *P. purdomii*, *A. fabri* and *Picea brachytyla* are the dominant species at the 80-year stage, and the coniferous *P. brachytyla* and *A. fabri* are the dominant species at the 120-year stage. The approximate age of each stage was calibrated according to tree-rings and soil erosion rates assessed by ¹³⁷Cs method. A seven-scale chronosequence (from ca. 3 years to ca. 120 years) was used.

2.2. Soil and plant sampling

In August 2015, we sampled three 10×10 m square plots with a distance of 10 m between plots (except for stages 1 and 2 with 5×5 m square plots and a 3-m distance between plots due to the small area at the early stages) at each chronosequence stage. For soil samples, five soil cores to a depth of 20 cm were collected from the center and each corner in each plot using a 5-cm diameter soil corer after removing surface litter by hand. The five soil cores collected at each stage were combined and homogenized to form one composite soil sample. The composite samples were stored in polyethylene bags with labels and transported to the laboratory with ice coolers. Once in the laboratory, soil samples were passed through a 2-mm sieve, and roots and stones were picked out. Approximately 500 g soil was divided into three parts and the material was used for (1) an analysis of soil physicochemical properties (air dried), (2) assays of soil extracellular enzymes activities and GRSP contents (stored at -20°C for no more than two weeks), and (3) an estimation of soil microbial biomass and communities (stored at -80°C). In each plot, all plant taxa were listed at the species level to assess the composition and richness of the plant community, including the tree, shrub and herb layers. If higher than 3 m, the tree biomass was calculated with the allometric equations reported by Zhong et al. (1997). The biomass of the shrub and herb layers and smaller trees was obtained through destructive sampling within the central 2×2 m area of each subplot (Yang et al., 2014). Plant litter samples were collected using 1-mm mesh litter traps with collection area of 0.42 m^2 , at >0.5 m high from the ground to avoid tidal water. The litter traps were emptied monthly and individual litter components were dried at 80°C for 48 h, desiccated at room temperature and weighed. All sampled plant materials were sorted by species, and then oven-dried and weighted.

2.3. Physiochemical analysis and GRSP determination

All litter samples were cleaned and oven-dried at 60 °C for 72 h before the final dry weight was recorded (Lei et al., 2015). Soil moisture (SM) was measured by drying 15 g fresh soil at 105 °C for 48 h. The soil pH was measured in each soil sample by a platinum black electrode and a glass electrode in a 1:10 (w/v weight:volume) aqueous solution, and the soil bulk density (SD) was quantified (Maynard and Curran, 2006; Lei et al., 2015). Soil total P (TP) was digested with nitric-perchloric acid (HClO₄), then measured with the molybdate colorimetric method (Murphy and Riley, 1962) using a UV2450 (Shimadzu, Japan). Soil available P (SAP) was sequentially extracted with 1 M MgCl₂, 0.5 M NH₄F, 0.1 M NaOH-0.5 M Na₂CO₃, and 1 M HCl. The soil samples were shaken end-over-end in 50-ml centrifuge tubes with 30 ml reagent for 16 h at 25 °C and 250 rpm. All extracts were centrifuged at 6000×g for 20 min at 0 °C, before the supernatant was decanted for the analysis of PO₄³⁻-P. Concentrations of PO₄³⁻-P in all extracts were determined using the Murphy and Riley (1962) method on a UV-VIS spectrophotometer (Shimadzu UV2450) at 710 nm. Total soil nitrogen (TN) was measured with a Kjeltac 2200 Auto Distillation Unit (FOSS Tecator, Sweden) by the semimicro-Kjeldahl method. Soil organic carbon (SOC) was determined by wet combustion (Nelson and Sommers, 1982). The soil dissolved nitrogen (SDN) was determined by persulfate oxidation with subsequent nitrate measurements. Briefly, concentrations of SDN, the sum of dissolved organic and inorganic nitrogen, were measured in 0.5 mol L⁻¹ K₂SO₄ extracts by the determination of NO₃⁻ following persulfate digestion (oxidation) of NH₄⁺ and organic N to NO₃⁻. In addition, soil microbial C, N and P concentrations were determined using a chloroform fumigation extraction method (Brookes et al., 1985).

Easily extractable and total glomalin (EE-GRSP and T-GRSP) were extracted according to the protocol described in detail by Zhang et al. (2015, 2017) and then measured by the Bradford protein assay (Wright

208 and Upadhyaya, 1996). 1 g of 2-mm sieved soil was used for EE-GRSP or T-GRSP extractions using 8 mL
209 of 20 mmol L⁻¹ sodium citrate (pH = 7.0) or 50 mmol L⁻¹ of sodium citrate (pH = 8.0). The soil extractions
210 were autoclaved for 30 (EE-GRSP) or 60 (T-GRSP) min at 121 °C, after which the supernatant was removed
211 by centrifugation at 10,000 × g for 10 min. The T-GRSP extraction was performed 4 times until the solution
212 was straw-colored. The supernatants were pooled and stored at 4 °C until the Bradford analysis (Wright and
213 Upadhyaya, 1996; Rillig, 2004). An enzyme microplate reader (Thermo Multiskan FC, USA) was used to
214 read the optical density value of GRSP at 595 nm using bovine serum albumin as a standard. The
215 contribution of GRSP to SOC was revealed by the GRSP/SOC ratio.

216

217 2.4. Extracellular enzyme activities: extraction and determination

218

219 At each plot, we measured the activities of six extracellular soil enzymes, including β-1,4-glucosidase (BG),
220 cellobiosidase (CBH), peroxidase (POX), β-1,4-N-acetyl-glucosaminidase (NAG), leucine amino-peptidase
221 (LAP) and acid phosphatase (AP). The list of enzymes that were assayed and their corresponding substrates
222 are presented in table S1. The method was described in detail by Jing et al. (2017). In short, we used a
223 96-well fluorometric microplate to determine soil enzymes activities. For hydrolytic enzymes (e.g., BG,
224 NAG, LAP, AP and CBH), 1.5 g fresh soil was weighted and suspended in a 1 mM sodium acetate buffer,
225 4-methylumbelliferone (MUB) standards, and MUB (fluorescently) labeled substrates. For peroxidase, 1.5 g
226 fresh soil was weighted and suspended in a 1 mM sodium acetate buffer and L-3,4-dihydroxyphenylalanine
227 (L-DOPA). Hydrolytic enzymes were measured with 8 replicates for 2.5 h, and peroxidase with 8 replicates
228 for 24 h in the dark at 25 °C. Then, the hydrolytic enzyme activities were assessed by evaluating
229 fluorescence at 360 nm excitation and 460 nm emission, and peroxidase at 450 nm in a microplate reader
230 (Thermo Lab systems, Franklin, MA, USA).

2.5. Microbial biomass and community composition

Phospholipid fatty acids (PLFAs) were determined to assess the structure of soil microbial communities at each plot using the method of Frostegård et al. (1991). Briefly, 5 g of soil of each sample (fresh weight) was extracted twice using the one-phase mixture of chloroform, methanol and citrate acid buffer (1:2:0.8, v/v/v). Lipids were separated into neutral lipids, glycolipids and phospholipids by chromatography on silicic acid columns. Then, the phospholipids were transformed by alkaline methanolysis into fatty methylesters, which were analyzed and quantified by a Hewlette-Packard 6890N-5973N Gas Chromatograph fitted with a 25 m capillary column (Agilent 25 m × 0.2 mm inner diameter × 0.33 µm film thickness), using hydrogen as the carrier gas and N as the makeup gas. The gas chromatography conditions were set by the MIDI Sherlock program (MIDI, Inc. Newark, DE). All fatty acids were given in the table S3. The abundance of individual fatty acid methyl esters was recorded as nmol PLFA g⁻¹ soil. The bacterial and fungal biomass was estimated as the sums of bacterial PLFAs and fungal PLFAs, respectively. The fungi-to-bacteria ratio (F/B) was calculated from the respective sums of the above bacterial and fungal PLFA markers.

2.6. Statistical analyses

The changes in biomass, and ratios of G⁺/G⁻ and fungal/bacterial PLFAs were subjected to one-way analyses of variance (ANOVA) to determine the overall effects of chronosequence stages using SPSS 19.0 (SPSS Inc., Chicago, IL). Significant differences among means were evaluated by Tukey's honest significant difference (HSD) at $p < 0.05$. The regression analysis between glomalin (including T-GRSP and EE-GRSP) and six extracellular soil enzymes were also performed using SPSS 19.0. The C:N, C:P, and N:P acquisition ratios

were presented as $\ln(\text{BG}+\text{CBH}):\ln(\text{NAG}+\text{LAP}):\ln(\text{AP})$ activities (Sinsabaugh et al., 2008). On the other hand, stoichiometric analyses of the soil enzyme data were conducted using the methods of Chen et al. (2018) to calculate enzyme ratios, threshold elemental ratios (TER), and lignocelluloses indices (LCI). TER for C:N and C:P was calculated according to Sinsabaugh et al. (2009):

$$\text{TER}_{\text{C:N}} = ((\text{BG}+\text{CBH})/(\text{NAG}+\text{LAP})) \times B_{\text{C:N}}/n_0 \quad \text{eqn 1}$$

$$\text{TER}_{\text{C:P}} = ((\text{BG}+\text{CBH})/(\text{NAG}+\text{LAP})) \times B_{\text{C:P}}/p_0 \quad \text{eqn 2}$$

When $\text{TER}_{\text{C:N}}$ and $\text{TER}_{\text{C:P}}$ are the threshold ratios (dimensionless), $B_{\text{C:N}}$ and $B_{\text{C:P}}$ represent the microbial biomass C:N or C:P ratios. The normalization constants n_0 and p_0 are the intercepts of the regressions for $\ln(\text{BG}+\text{CBH})$ vs. $\ln(\text{NAG} + \text{LAP})$ and $\ln(\text{BG}+\text{CBH})$ vs. $\ln(\text{AP})$ respectively. TER was used to reflect microbial resource limitation by comparing it to the available soil C:N or C:P ratio. If C:N or C:P was greater than TER for an element, the result suggested resource limitation (Sturner and Elser, 2002). Significant differences between C:N or C:P ratios and threshold ratios are estimated by simple T-test at each successional stage.

Furthermore, according to the approach of Tapia-Torres et al. (2015), the substrate C quality can be determined by the enzyme-based lignocelluloses index (LCI). Higher LCI indicates lower quality substrate C:

$$\text{LCI} = \ln \text{POX} / (\ln \text{POX} + \ln \text{BG}) \quad \text{eqn 3}$$

To further investigate the effects of variables on the composition of soil microbes and on the activities of soil extracellular enzymes, the redundancy discriminatory analysis (RDA) in the *vegan* R package was used (R Development Core Team, 2016). Before RDA, we used a forward selection procedure to select environmental factors (Blanchet et al., 2008). All significant ($p < 0.05$) variables were selected and used in further analyses. Furthermore, to visualize the complex relationships among variables, we performed

structural equation modeling (SEM) to estimate the direct and indirect effects determining available C, N and P in soil (Grace et al., 2010). According to the method of Wang et al. (2018), we classified all variables into five groups, including soil environment (pH, SD and SM), vegetation (plant richness, PR; plant litter biomass, PL; and total above-ground biomass, TAB), eco-enzymatic stoichiometry (BG, CBH, NAG, LAP, AP and POX), soil microbial structures (T-PLFA, Bact, Fungi and Acti) and Glomalin-related soil protein (T- and EE-GRSP). Before the SEM analysis, a principal components analysis (PCA) was performed to create a multivariate index representing each group to exclude the variables' autocorrelation (Wang et al., 2018). Within each group, only variables that were significantly correlated with soil available C, N and P were included in PCA. The first principal component (PC1), which explained 67-91% of the total variance for each group, was subsequently used in the SEM analysis. All included factors were subjected to logarithmic transformation to meet the assumptions of normality. The SEM analysis was conducted with the Amos 17.0 software package (Smallwaters Corporation, Chicago, IL, USA). The criteria for the evaluation of structural equation modeling fit, such as the *p*-values, χ^2 values, goodness-of-fit index (GFI) and the root mean square error of approximation (RMSEA), were adopted according to Grace et al. (2010).

3. Results

3.1. Microbial dynamics and GRSP accumulation

Along the chronosequence, the microbial biomass, as indicated by PLFAs, showed clear variation with soil age (Table S2; Fig.1). Total PLFAs, fungi, G^+ and G^- PLFAs (Fig. 1a-d) were found to increase significantly with soil age, except for the 40-year stage. The G^+/G^- ratios significantly increased along the successional stages, reaching a peak at the middle stages (Fig. 1e). Furthermore, the fungi to bacteria ratios were lowest at the 12-year stage and highest at later stages (80-120 years) (Fig. 1f).

The concentrations of both easily extractable and total glomalin-related soil proteins (EE-GRSP and T-GRSP) increased significantly with the soil age (Fig. 2a, b). During the first four stages, the ratio of EE-GRSP/T-GRSP increased to 53.3% and then remained at that level during the last three stages (data not shown). However, their contributions to SOC increased linearly from 0.9 to 2.6% for EE-GRSP and from 2.4 to 5.9% for T-GRSP (Fig. 2c, d). The concentrations of T-GRSP and EE-GRSP increased linearly as a function of the AMF content (Fig. 2e, f).

3.2. Eoenzymatic stoichiometry and potential nutrient limitation

Extracellular enzymes activities of soil increased dramatically along the successional stages following the glacial retreat (Fig. S1). Potential C, N and P acquiring activities were significantly correlated with each other, and the overall slope of C:N, C:P and N:P activity regressions were 0.67, 0.69 and 0.90, respectively (Fig. 3a-c). At the 3-year stage, microbial activities showed a higher investment in BG + CBH and NAG +

LAP enzymes than in the AP enzyme, while at the 40-120 years stages, microbes tended to have a higher investment in P-acquiring enzymes (Fig. 3a-c). This pattern was further supported by the microbial stoichiometric analyses, which indicated the presence of a potential C and N co-limitation at the early stages, then mainly P limitation at the late stages (Fig. 3d).

TER_{C:N} and TER_{C:P} were stable during four early successional stages but increased significantly during the later stages (Fig. 4a, b). In addition, TER_{C:N} was lower than available C:N (e.g. SOC:SDN) across the chronosequence, except for the first stage (3 years), while TER_{C:P} was higher than available C:P (e.g. SOC:SAP) during the four early stages (3-40 years) and lower than available C:P at the last three stages (52-120 years) (Fig. 4a, b). Moreover, the enzyme-based LCI index significantly decreased during the early three stages and maintained its lower level at the 30-120 -year stages (Fig. 4c). The concentrations of T-GRSP and EE-GRSP exhibited a linear increase with soil C-, N- and P-hydrolyzing enzymes activities along the chronosequence (Fig. 5).

3.3. The relative contributions of edaphic and biotic factors to soil microbial processes

The redundancy analysis (RDA) showed that the microbial community structure could be differentiated into three clusters: 3-12 (cluster 1), 30-52 years (cluster 2), and 80-120 years (cluster 3) (Fig. 6a). The soil extracellular enzyme activities could also be differentiated into three clusters: 3 years (cluster 1), 12 years (cluster 2), and 30-120 years (cluster 3) (Fig. 6b). Furthermore, T-PLFA and F-PLFA were best explained by vegetation characteristics, including the total aboveground and plant litter biomass, as well as soil physicochemical properties, including soil available phosphorus and dissolved nitrogen (SAP and SDN). However, B-PLFA was tightly related to SOC, and the ratios of F/B and G⁺/G⁻ were best accounted by pH

and soil density (Fig. 6a). The activities of C-hydrolyzing enzymes (BG and CBH) were closely correlated with SOC, SDN, SAP and GRSP. Nitrogen-acquiring NAG and LAP were negatively related with SDN. Acid phosphatase was positively correlated with SAP and MBP, but negatively with pH and soil density. Peroxidase was negatively correlated with vegetation characteristics, including plant richness, and the aboveground and litter biomass (Fig. 6b).

The SEM models well fit the significance criteria according to their χ^2 , *P*, AIC, GFI and RMSEA values (Fig. 7a, b). At the early stages (3-52 years), environmental factors caused a greater impact on microbial communities and enzyme stoichiometry, while at the late stages (80-120 years), biotic vegetation properties as well as PLFAs began to dominate (Fig. 7a, b). GRSP contributed to SOC accumulation more at the late stages than at the early stages. Moreover, eco-enzymatic stoichiometry was tightly related to SAP at the late stages, while no significant relationship was detected at the early stages (Fig. 7).

4. Discussion

Microbial communities are the main drivers of organic matter decomposition to expedite pedogenesis, to facilitate the establishment of vascular plants, and to accelerate the successional dynamics of ecosystems, especially in pristine environments, such as glacier retreat areas (Bradley et al., 2016; Castle et al., 2017). According to our previous survey, plant growth in the *Hailuoguo Glacier Chronosequence* area is most often N-limited at early successional stages, whereas often limited by P availability at older, more developed stages (Jiang et al., 2018). However, the understanding of the sequence and magnitude of changes in the microbial community assembly, as well as of the mechanistic underpinnings of microbial contributions to pedogenic development is still highly fragmentary. In addition, it is not well understood, whether generalizable patterns of nutrient limitation are applicable to metabolically and phylogenetically diverse soil microbial communities. Therefore, soil microbial biomass and community structures, GRSP (EE- and T-GRSP) concentrations and the stoichiometry of extracellular enzymes, which are reliable indicators of the biological condition of soil (Gispert et al., 2013; Zhang et al., 2017), were now quantified during the primary succession across the *Hailuoguo Glacier Chronosequence*.

4.1. Microbial community dynamics and GRSP accumulation along the chronosequence

The seven stages of the 120-year succession were separated into three distinct clusters for microbial communities (Figs. 1, 6). Also, the fungi/bacteria ratio was lowest at the 12-year stage and reached its highest level at the last two stages (80-120 years) (Fig. 1f). In agreement with the present study, Fernández-Martínez et al. (2017) reported most important roles for bacteria at the initial stages of succession, while dominant roles for saprophytic and mycorrhizal fungi as succession progressed along a glacier

forefield. The pattern coincided with the vegetation dynamics, as broadleaved shrubs and trees dominate at stages 1-5, and coniferous *Abies fabri* and *Picea brachytyla* trees at stages 6 and 7 (Lei et al., 2015). Several studies have proposed that there is a shift from an early bacterial dominance to a late fungal dominance when plant establishment becomes increasingly important (Sun et al., 2016; Yoshitake et al., 2018). Besides serving as immediate decomposers, a large proportion of fungi can act as endophytes, mutualists or pathogens. Therefore, a strong coupling of plant-fungal distribution patterns would be expected at regional scales (Wardle, 2004; Chen et al., 2017; Jiang et al., 2018), which is supported also by the correlation between plant species richness and litter biomass, and fungal PLFA (Fig. 6a).

Glomalin-related soil proteins (GRSP), products of arbuscular mycorrhizal fungi deposited into soil after hyphae senesce (Treseder and Turner, 2007) can account for 4–5% of soil C, which exceeds the 0.08-0.2% contribution from soil microbial biomass (Rillig et al., 2001). In the *Hailuoguo Glacier Chronosequence*, the concentrations of both easily extractable and total GRSP increased significantly with the soil age (Fig. 2a, b). These results are consistent with some previous works conducted in other tropical locations, where the GRSP content improved with an increasing plants density and vegetation complexity (Singh et al., 2013; Kumar et al., 2018). In addition, their contributions to SOC increased linearly from 0.9% to 2.6% for EE-GRSP and from 2.4% to 5.9% for T-GRSP (Fig. 2c, d). Moreover, the concentrations of T-GRSP and EE-GRSP increased linearly as a function of the AMF content (Fig. 2e, f), thus implying the importance of fungi at late stages. On the other hand, the sticky nature of GRSP enables it to protect organic matter from decomposition by promoting the formation of soil aggregates (Rillig et al., 2003; Rillig, 2004). Overall, these results demonstrated that both GRSP fractions in soil might be two reliable indicators during pedogenic development, particularly under environmental change scenarios.

4.2. Ecoenzymatic stoichiometry and potential nutrient limitation along the chronosequence

Extracellular enzyme activities can effectively reflect the functions of decomposer communities depending on the dynamic balance of metabolic requirements and nutrient availability (Adamczyk et al., 2014; Yang and Zhu, 2015; Cui et al., 2018). Along the chronosequence, an environment with a higher carbon content supports more developed and persistent plant communities that can provide a longer-term buildup of soil organic matter (Lei et al., 2015), which was found to result in stronger microbial metabolism and more effective extracellular enzymes for N and P acquisition (Figs. S1 and 3). At the later stages with the establishment of coniferous trees, POX activities increased significantly at higher decomposition rates of non-labile SOC, because POX is an enzyme for decomposing recalcitrant C fractions, such as lignin and humus (Fig. S1f, Sinsabaugh, 2011). In addition, the higher decomposition rate of labile SOC was evident based on the higher BG activity and lower LCI during later stages (Fig. S1c and Fig 4c). Higher BG indicated that more C-acquisition enzymes were produced for decomposing the labile SOC fraction. Yoshitake et al. (2018) found that the accumulation of soil organic C in a glacier foreland is known to be strongly affected by the vegetation cover.

In the present study, fungal biomass and F/B ratio were higher in soils with *A. fabri* and *P. brachytyla* during later successional stages (Fig. 1b, f). These results indicate that the establishment of coniferous trees has a great impact, especially on the fungal community. These coniferous trees are mycorrhizal species and, therefore, the direct effect of symbiotic fungi is not negligible in this case. Indeed, higher mycorrhizal richness favors plants productivity by improving the availability of nutrients from the soil environment. Moreover, roots and mycorrhizal fungi can also enhance SOM decomposition. Roots release exudates to soil and provide carbohydrates to mycorrhizal fungi, and both processes provide heterotrophic microbes with the

energy needed to synthesise extracellular enzymes to degrade SOM (Phillips et al., 2012). Roots and mycorrhizal fungi, for example, promote root- and mycorrhizal-derived C entering forest soils rapidly under elevated CO₂ cycles, which limits soil C accumulation and increases N cycling rates (Phillips et al., 2012). This suggests that possible differences in litter quality, root exudates, mycorrhizal fungi and supply of rhizodeposits from plant roots might affect the supply of organic C.

Microbial extracellular enzyme stoichiometry has been suggested as a useful indicator in revealing nutrient constraints of microbial assemblages in response to environmental resource availability (Chen et al., 2018). In the Hailuoguo chronosequence, available C:N was higher than TER_{C:N} during all stages (Fig. 4a), indicating that microbial activities might be N-limited due to young pedogenesis. Furthermore, at the first stage, a higher investment in the BG+CBH and NAG+LAP enzymes relative to the AP enzyme was observed (Fig. 3), which suggested that microbial activity was co-limited by C and N after three-year deglaciation. Conversely, microbial activities were limited by P at the late stages (80–120 years), as shown by the higher investment in AP relative to the BG and CBH enzymes (Fig. 3b). The higher available C:P ratio compared to TER_{C:P} during the late succession stages (Fig. 4b) also suggested that microbial activities were then more P-limited compared to the early stage.

Based on the unique global P cycle, Walker and Syers (1976) predicted that P fractions are transformed into more stable forms, resulting in P becoming the limiting nutrient and ecosystem component in extreme situations. At the *Hailuoguo Glacier Chronosequence*, the P loss was observed after 52 years of deglaciation, and the loss reached 12.9% and 17.6% on the 80- and 120-year-old sites, respectively, approximately 7 times the level detected at the 110-year-old Rakata chronosequence (Schlesinger et al., 1998; Wu et al., 2015). The fast loss of P from the soil could be attributed to the higher weathering rate, the large amount of

plant uptake and transport by run-off. In addition to being assimilated by plants, the released phosphate tends to be adsorbed onto the surface of Fe and Al hydroxides due to the sharp decrease in pH, accounting for more than 30% of the total P at the 80- and 120-year-old sites (Zhou et al., 2016). However, the elevation difference of 150 m along less than 2 km of the Hailuoguo chronosequence, as well as the abundant annual precipitation (approximately 1,947 mm) led to a strong erosion and great loss of soil P. Thus, the P availability may become a limited resource for microbial activities in the studied chronosequence within a century of initial soil formation.

4.3. The relative contributions of edaphic and biotic factors to microbial processes

The SEM models showed that at the early stages, soil environmental factors caused a great impact on microbial communities and enzymes stoichiometry (Fig. 7a). Given that soil directly provides the substrate and environment for microbial communities, the edaphic properties are expected to be more important in shaping the microbial dynamics. In Tibetan alpine grasslands, Chen et al. (2017) found that variation in soil microbial communities are mainly explained by edaphic factors, including soil organic carbon, C:N ratio, pH and soil texture. On the other hand, the explaining capacity of biotic factors increased at the last two stages along with the increasingly important forest cover (Fig. 7b), coincident with the establishment of a coniferous forest (Lei et al., 2015), high aboveground and litter biomass accumulation and a low litter quality (Table S2). Our previous results have also suggested that plants govern the turnover of soil fungal communities and functional characteristics in the Hailuoguo chronosequence, likely due to the continuous input of detritus and differences in litter biochemistry among plant species (Jiang et al., 2018). The present study further demonstrated that vegetation might play an important role in determining the ecoenzymatic stoichiometry of soil, probably through direct effects on root systems (secreting exoenzymes) and indirect

effects on root systems (affecting microbial rhizosphere communities).

5. Conclusions

In this study, we investigated soil microbial community structures, soil enzyme activities and GRSP, and disentangled the nutrient limitation of microbial successional trajectories along the *Hailuoguo Glacier Chronosequence*. The microbial biomass increased significantly with soil age until reaching the maximum at late stages. In addition, the microbial communities exhibited a distinct shift from a bacterial to fungal dominated pattern across the glacier chronosequence. On the basis of ecoenzymatic stoichiometry and threshold elemental ratio analyses, we found that microbial resource limitation was different along the chronosequence. At early successional stages, microbial activities were more carbon and nitrogen limited than at late stages, while phosphorus-limited phenomena became more serious with the rapid loss of phosphate at the late stages. Moreover, the redundancy analysis and structural equation modeling suggested that the edaphic factors are the primary agents influencing microbial processes, especially at the early stages, and the explaining capacity of vegetation factors increased during the last two stages along with the increasing importance of forest cover. Altogether, these findings provide useful knowledge of understanding soil-plant-microbe interactions and soil biogeochemical cycles during ecosystem successions. Nevertheless, we focused only on the relatively important environmental variables. Some unmeasured factors related to microbial community structures, such as root biomass, were not estimated in the present study. In future studies, it is important to ascertain whole-community level genetic factors responsible for nutrient transformation *in situ* through metagenomics, in order to obtain a more complete picture of the underlying mechanisms of microbial feedbacks to ecosystem succession under environmental changes.

Acknowledgements This work was supported by the National Science Foundation of China (31570598,

31500505) and the Talent Program of the Hangzhou Normal University (2016QDL020).

References

509

Adamczyk, B., Kilpeläinen, P., Kitunen, V., Smolander, A., 2014. Potential activities of enzymes involved in N, C, P and S cycling in boreal forest soil under different tree species. *Pedobiologia* 57, 97-102.

Blanchet, F.G., Legendre, P., Borcard, D., 2008. Forward selection of explanatory variables. *Ecology* 89, 2623-2632.

Bradley, J.A., Arndt, S., Šabacká, M., Benning, L.G., Barker, G.L., Blacker, J.J., Yallop, M.L., Wright, K.E., Bellas, C.M., Telling, J., Tranter, M., Anesio, A.M., 2016. Microbial dynamics in a high-arctic glacier forefield: a combined field, laboratory, and modeling approach. *Biogeosciences* 13, 5677-5696.

Brookes, P.C., Landman, A., Pruden, G., Jenkinson, D.S., 1985. Chloroform fumigation and the release of soil N: a rapid direct extraction method to measure microbial biomass N in soil. *Soil Biol. Biochem.* 17, 837-842.

Camenzind, T., Hättenschwiler, S., Treseder, K.K., Lehmann, A., Rillig, M.C., 2017. Nutrient limitation of soil microbial processes in tropical forests. *Ecol. Monogr.* 88, 4-21.

Castle, S.C., Sullivan, B.W., Knelman, J., Hood, E., Nemergut, D.R., Schmidt, S.K., Cleveland, C.C., 2017. Nutrient limitation of soil microbial activity during the earliest stages of ecosystem development. *Oecologia* 185, 513-524.

Chen, H., Li, D., Xiao, K., Wang, K. 2018. Soil microbial processes and resource limitation in karst and non-karst forests. *Funct. Ecol.* 32, 1400-1409.

Chen, Y., Xu, T., Veresoglou, S.D., Hu, H., Hao, Z., Hu, Y., Liu, L., Deng, Y., Rillig, M.C., Chen, B., 2017. Plant diversity represents the prevalent determinant of soil fungal community structure across temperate grasslands in northern China. *Soil Biol. Biochem.* 110, 12-21.

530 Cui, Y., Fang, L., Guo, X., Wang, X., Zhang, Y., Li, P., Zhang, X., 2018. Ecoenzymatic stoichiometry and
531 microbial nutrient limitation in rhizosphere soil in the arid area of the northern Loess Plateau, China.
532 Soil Biol. Biochem. 116, 11-21.

533 Fernández-Martínez, M.A., Pérez-Ortega, S., Pointing, S.B., Allan Green, T.G., Pintado, A., Rozzi, R.,
534 Sancho, L.G., de los Ríos, A., 2017. Microbial succession dynamics along glacier forefield
535 chronosequences in Tierra del Fuego (Chile). Polar Biol. 40, 1939-1957.

536 Frostegård, Å., Tunlid, A., Bååth, E., 1991. Microbial biomass measured as total lipid phosphate in soils of
537 different organic content. J. Microbiol. Meth. 14, 151-163.

538 Gispert, M., Emran, M., Pardini, G., Doni, S., Ceccanti, B., 2013. The impact of land management and
539 abandonment on soil enzymatic activity, glomalin content and aggregate stability. Geoderma 202-203,
540 51-61.

541 Grace, J.B., Anderson, T.M., Olff, H., Scheiner, S.M., 2010. On the specification of structural equation
542 models for ecological systems. Ecol. Monogr. 80, 67-87.

543 Hill, B.H., Elonen, C.M., Seifert, L.R., May, A.A., Tarquinio, E., 2012. Microbial enzyme stoichiometry and
544 nutrient limitation in US streams and rivers. Ecol. Indic. 18, 540-551.

545 Insam, H., Delgado-Granados, H., Nagler, M., Waldhuber, S., Podmirseg, S.M., Quideau, S., 2017. Soil
546 microbiota along Ayoloco glacier retreat area of Iztaccíhuatl volcano, Mexico. Catena 153, 83-88.

547 Jiang, Y., Lei, Y., Yang, Y., Korpelainen, H., Niinemets, Ü., Li, C., 2018. Divergent assemblage patterns and
548 driving forces for bacterial and fungal communities along a glacier forefield chronosequence. Soil Biol.
549 Biochem. 118, 207-216.

550 Jing, X., Chen, X., Tang, M., Ding, Z., Jiang, L., Li, P., Ma, S., Tian, D., Xu, L., Zhu, J., Ji, C., Shen, H.,
551 Zheng, C., Fang, J., Zhu, B., 2017. Nitrogen deposition has minor effect on soil extracellular enzyme
552 activities in six Chinese forests. Sci. Total Environ. 607-608, 806-815.

553 Knelman, J.E., Legg, T.M., O'Neill, S.P., Washenberger, C.L., González, A., Cleveland, C.C., Nemergut,
554 D.R., 2012. Bacterial community structure and function change in association with colonizer plants
555 during early primary succession in a glacier forefield. *Soil Biol. Biochem.* 46, 172-180.

556 Kumar, S., Singh, A.K., Ghosh, P., 2018. Distribution of soil organic carbon and glomalin related soil
557 protein in reclaimed coal mine-land chronosequence under tropical condition. *Sci. Total Env.* 625,
558 1341-1350.

559 Lei, Y., Zhou, J., Xiao, H., Duan, B., Wu, Y., Korpelainen, H., Li, C., 2015. Soil nematode assemblages as
560 bioindicators of primary succession along a 120-year-old chronosequence on the Hailuoguo Glacier
561 forefield, SW China. *Soil Biol. Biochem.* 88, 362-371.

562 Lovelock, C.E., Wright, S.F., Clark, D.A., Ruess, R.W., 2004. Soil stocks of glomalin produced by
563 arbuscular mycorrhizal fungi across a tropical rain forest landscape. *J. Ecol.* 92, 278-287.

564 Matthews, J.A., 1992. The ecology of recently-deglaciated terrain: a geoecological approach to glacier
565 forelands and primary succession. Cambridge University Press, Cambridge.

566 Maynard, D.G., Curran, M.P., 2006. Soil density measurement in forest soils. In: Carter MR, Gregorich EG
567 (Eds.), *Soil Sampling and Methods of Analysis*, second edn. CRC Press, pp. 863-869.

568 Murphy, J., Riley, J.P., 1962. A modified single solution method for determination of phosphate in natural
569 waters. *Anal. Chim. Acta* 26, 31-36.

570 Nelson, D.W., Sommers, L.E., 1982. Total carbon, organic carbon and organic matter. In: Page, A.L., Miller,
571 R.H., Keeney, D.R. (Eds.), *Methods of Soil Analysis*. American Society of Agronomy, Madison, Wis,
572 pp. 539-579.

573 Peng, X.Q., Wang, W., 2016. Stoichiometry of soil extracellular enzyme activity along a climatic transect in
574 temperate grasslands of northern China. *Soil Biol. Biochem.* 98, 74-84.

575 Phillips, R.P., Meier, I.C., Bernhardt, E.S., Grandy, A.S., Wickings, K., Finzi, A.C., 2012. Roots and fungi

576 accelerate carbon and nitrogen cycling in forests exposed to elevated CO₂. *Ecol. Lett.* 15, 1042-1049.

577 R Development Core Team, 2016. R: A Language and Environment for Statistical Computing. R Foundation
578 for Statistical Computing, Vienna, Austria <https://www.R-project.org> (ISBN 3-900051-07-0).

579 Rillig, M., Wright, S., Nichols, K., Schmidt, W., Torn, M., 2001. Large contribution of arbuscular
580 mycorrhizal fungi to soil carbon pools in tropical forest soils. *Plant Soil* 233, 167-177.

581 Rillig, M.C., 2004. Arbuscular mycorrhizae, glomalin, and soil aggregation. *Can. J. Soil Sci.* 84, 355-363.

582 Rillig, M.C., Ramsey, P.W., Morris, S., Paul, E.A., 2003. Glomalin, an arbuscular mycorrhizal fungal soil
583 protein, responds to land-use change. *Plant Soil* 253, 293-299.

584 Schindler, F.V., Mercer, E.J., Rice, J.A., 2007. Chemical characteristics of glomalin-related soil protein
585 (GRSP) extracted from soils of varying organic matter content. *Soil Biol. Biochem.* 39, 320-329.

586 Schlesinger, W.H., Bruijnzeel, L.A., Bush, M.B., Klein, E.M., Mace, K.A., Raikes, J.A., Whittaker, R.J.,
587 1998. The biogeochemistry of phosphorus after the first century of soil development on Rakata Island,
588 Krakatau, Indonesia. *Biogeochemistry* 40, 37-55.

589 Schmidt, S.K., Porazinska, D., Concienne, B.L., Darcy, J.L., King, A.J., Nemergut, D.R., 2016.
590 Biogeochemical stoichiometry reveals P and N limitation across the post-glacial landscape of Denali
591 National Park, Alaska. *Ecosystems* 19, 1164-1177.

592 Singh, P.K., Singh, M., Tripathi, B.N., 2013. Glomalin: an arbuscular mycorrhizal fungal soil protein.
593 *Protoplasma* 250, 663-669.

594 Sinsabaugh, R.L., Hill, B.H., Shah, J.J.F., 2009. Eoenzymatic stoichiometry of microbial organic nutrient
595 acquisition in soil and sediment. *Nature* 462, 795-798.

596 Sinsabaugh, R.L., Lauberaw, C.C.L., Weintraub, M.N., Ahmed, B., Allison, S.D., Crenshaw, C., Contosta,
597 A.R., Cusack, D., Frey, S., Gallo, M.E., Gartner, T.B., Hobbie, S.E., Holland, K., Keeler, B.L., Powers,
598 J.S., Stursova, M.S., Takacs-Vesbach, C., Waldrop, M.P., Wallenstein, M.D., Zak, D.R., Zeglin, L.H.,

2008. Stoichiometry of soil enzyme activity at global scale. *Ecol. Lett.* 11, 1252-126.

Smith, S.E., Read, D.J., 2008. *Mycorrhizal Symbiosis*. Academic Press, pp. 13-15.

Sørensen, L.I., Holmstrup, M., Maraldo, K., Christensen, S., Christensen, B., 2006. Soil fauna communities and microbial respiration in high Arctic tundra soils at Zackenberg, Northeast Greenland. *Polar Biol.* 29, 189-195.

Sterner, R.W., Elser, J.J., 2002. *Ecological stoichiometry: The biology of elements from molecules to the biosphere*. Princeton, NJ: Princeton University Press.

Sun, H., Wu, Y., Zhou, J., Bing, H., 2016. Variations of bacterial and fungal communities along a primary successional chronosequence in the Hailuoguo glacier retreat area (Gongga Mountain, SW China). *J. Mt. Sci.* 13, 1621-1631.

Tapia-Torres, Y., Elser, J.J., Souza, V., García-Oliva, F., 2015. Ecoenzymatic stoichiometry at the extremes: How microbes cope in an ultra-oligotrophic desert soil. *Soil Biol. Biochem.* 87, 34-42.

Treseder, K.K., Turner, K.M., 2007. Glomalin in ecosystems. *Soil Sci. Soc. Am. J.* 71, 1257-1266.

Walker, T.W., Syers, J.K., 1976. The fate of phosphorus during pedogenesis. *Geoderma* 15, 1-19.

Wang, J., Sun, J., Xia, J., He, N., Li, M., Niu, S., 2018. Soil and vegetation carbon turnover times from tropical to boreal forests. *Funct. Ecol.* 32, 71-82.

Wang, J., Wu, Y., Zhou, J., Bing, H., Sun, H., 2016. Carbon demand drives microbial mineralization of organic phosphorus during the early stage of soil development. *Biol. Fertil. Soils* 52, 825-839.

Wardle, D.A., Bardgett, R.D., Klironomos, J.N., Setälä, H., Van Der Putten, W.H., Wall, D.H., 2004. Ecological linkages between aboveground and belowground biota. *Science* 304, 1629-1633.

Waring, B.G., Weintraub, S.R., Sinsabaugh, R.L., 2013. Ecoenzymatic stoichiometry of microbial nutrient acquisition in tropical soils. *Biogeochemistry* 117, 101-113.

Wright, S.F., Upadhyaya, A., 1996. Extraction of an abundant and unusual protein from soil and comparison

with hyphal protein of arbuscular mycorrhizal fungi. *Soil Sci.* 161, 575-586.

Wu, Y., Zhou, J., Bing, H., Sun, H., Wang, J., 2015. Rapid loss of phosphorus during early pedogenesis along a glacier retreat chronosequence, Gongga Mountain (SW China). *Peer J*, 3, e1377.

Yang, K., Zhu, J., 2015. The effects of N and P additions on soil microbial properties in paired stands of temperate secondary forests and adjacent larch plantation in Northeast China. *Soil Biol Biochem.* 90, 80-86.

Yang, Y., Wang, G.X., Shen, H.H., Yang, Y., Cui, H.J., Liu, Q., 2014. Dynamics of carbon and nitrogen accumulation and C:N stoichiometry in a deciduous broadleaf forest of deglaciated terrain in the eastern Tibetan Plateau. *For. Ecol. Manage.* 312, 10-18.

Yoshitake, S., Uchida, M., Iimura, Y., Ohtsuka, T., Nakatsubo, T., 2018. Soil microbial succession along a chronosequence on a High Arctic glacier foreland, Ny-Ålesund, Svalbard: 10 years' change. *Polar Sci.* 16, 59-67.

Yoshitake, S., Uchida, M., Koizumi, H., Nakatsubo, T., 2007. Carbon and nitrogen limitation of soil microbial respiration in a High Arctic successional glacier foreland near Ny-Ålesund, Svalbard. *Polar Res.* 26, 22-30.

Zhang, J., Tang, X., He, X., Liu, J., 2015. Glomalin-related soil protein responses to elevated CO₂ and nitrogen addition in a subtropical forest: Potential consequences for soil carbon accumulation. *Soil Biol. Biochem.* 83, 142-149.

Zhang, J., Tang, X., Zhong, S., Yin, G., Gao, Y., He, X., 2017. Recalcitrant carbon components in glomalin-related soil protein facilitate soil organic carbon preservation in tropical forests. *Sci. Rep.* 7. doi:10.1038/s41598-017-02486-6.

Zhong, X., Luo, J., Wu, N., 1997. Researches of the forest ecosystems on Gongga Mountain. Chengdu University of Science and Technology Press, Chengdu.

Zhou, J., Bing, H., Wu, Y., Yang, Z., Wang, J., Sun, H., Luo, J., Liang, J., 2016. Rapid weathering processes of a 120-year-old chronosequence in the Hailuoguo Glacier foreland, Mt. Gongga, SW China. *Geoderma* 267, 78-91.

Zhou, J., Wu, Y., Prietzel, J., Bing, H., Yu, D., Sun, S., Luo, J., Sun, H., 2013. Changes of soil phosphorus speciation along a 120-year soil chronosequence in the Hailuoguo Glacier retreat area (Gongga Mountain, SW China). *Geoderma* 195-196, 251-259.

668

669 **Figure captions**

670

671 **Figure 1.** Sums (panels a-d) and ratios (panels e-f) of phospholipid fatty acids (PLFAs) in microbial groups
 672 in soil of different ages along the *Hailuogou Glacier Chronosequence*. Each value is the mean \pm SE (n=3).
 673 Different lowercase letters indicate significant differences according to Tukey's HSD test at a significance
 674 level of $p < 0.05$.

675

676 **Figure 2.** Temporal changes in glomalin-related soil proteins, including T-GRSP and EE-GRSP (a, b), their
 677 contribution to SOC (c, d) and correlation with arbuscular mycorrhizal fungi (AMF, e, f).

678

679 **Figure 3.** Regressions analyses of $\ln(\text{BG}+\text{CBH})$ vs $\ln(\text{AP})$, $\ln(\text{BG}+\text{CBH})$ vs $\ln(\text{NAG} + \text{LAP})$, and \ln
 680 $(\text{NAG} + \text{LAP})$ vs $\ln(\text{AP})$ (a, b, c). The solid line is the regression line, and the dashed line is the reference
 681 line with slope = 1. The solid regression line to the left from the 1:1 line suggests more resources devoted to
 682 the enzyme on the y-axis compared with the x-axis [e.g., $\ln(\text{NAG} + \text{LAP})$ compared to $\ln(\text{AP})$]. The
 683 regression line to the right from the 1:1 line suggests more resources devoted to the enzyme on the x-axis
 684 compared with the y-axis. Stoichiometry analysis of enzyme activities at seven successional stages along the
 685 *Hailuogou Glacier Chronosequence* (d). “★” successional age 3 years, “■” 12 years, “●” 30 years, “▲”
 686 40 years, “◆” 52 years, “□” 80 years, and “○” 120 years.

687

688 **Figure 4.** Comparisons of (a) threshold elemental ratio (TER) of C:N and available C:N ratio (i.e.,
 689 SOC:SDN), (b) TER of C:P and available C:P ratio (i.e. SOC:SAP), and (c) lignocelluloses index (LCI)
 690 among different successional stages. Each value is the mean \pm SE (n=3). Different uppercase letters indicate

691 significant differences ($p < 0.05$) for SOC:SDN and SOC:SAP values, and different lowercase letters
692 indicate significant differences for $TER_{C:N}$, $TER_{C:P}$ and LCI values among different successional stages
693 according to Tukey's HSD test. Different asterisks indicate significant differences between $TER_{C:N}$ and
694 SOC:SDN values, and between $TER_{C:P}$ and SOC:SAP values at the same successional stage according to
695 simple t-test. SOC, soil organic C; SDN, soil dissolved N; SAP, soil available P.

696

697 **Figure 5.** Relationships between glomalin-related soil proteins (including T-GRSP and EE-GRSP) and soil
698 extracellular enzymes along the *Hailuogou Glacier Chronosequence*. Closed cycles and open cycles
699 represent total glomalin (T-GRSP) and easily extractable glomalin (EE-GRSP), respectively.

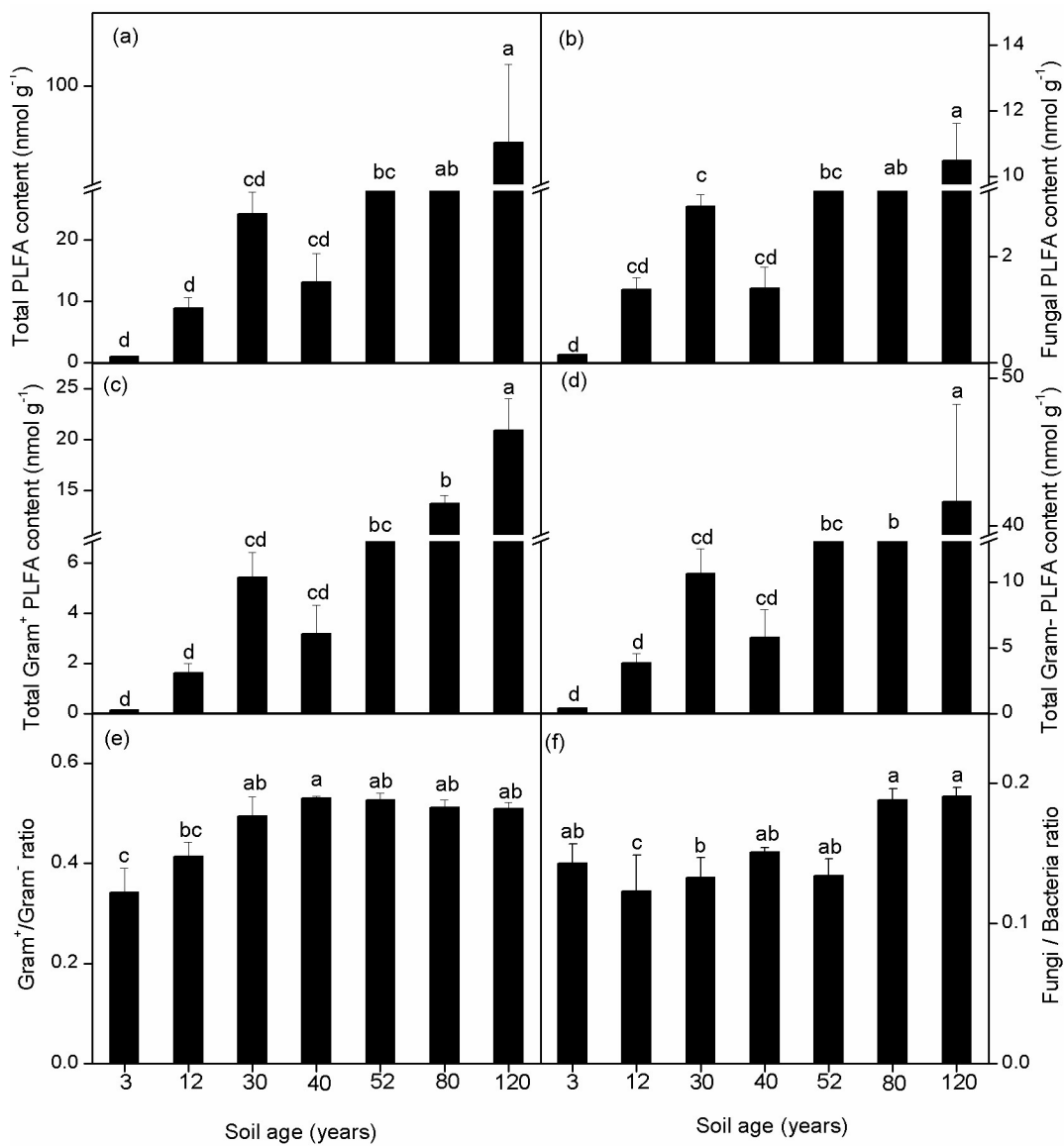
700

701 **Figure 6.** Redundancy analysis of selected environmental variables for microbial community structures (a)
702 and soil extracellular enzymes (b) along the *Hailuogou Glacier Chronosequence*. SOC, soil organic C; SDN,
703 soil dissolved N; SAP, soil available P; MBP, microbial P; PL, plant litter; PR, plant richness; TAB, total
704 above ground biomass; SM, soil moisture; SD, soil density; Stage codes as in Fig. 3.

705

706 **Figure 7.** Structure equation modeling depicting direct and indirect regulatory pathways of environmental
707 factors that affect microbial community structures, glomalin-related soil proteins and ecoenzymatic
708 stoichiometry at early (a) and late (b) successional stages along the *Hailuogou Glacier Chronosequence*.
709 Arrows represent positive (solid) or negative (dashed) path coefficients. Arrow width is proportional to the
710 strength of the relationship. Numbers on the arrows are standardized direct path coefficients. Double-layered
711 rectangles represent the first component of PCA conducted for soil environment, vegetation,
712 glomalin-related soil proteins, soil microbial characteristics and ecoenzymatic stoichiometry. The dark solid
713 “↑” and dashed “↓” symbols indicate a positive or negative relationship between the variables,

714 respectively. *, $p < 0.05$; **, $p < 0.01$; ***, $p < 0.001$.



715

716 **Figure 1**

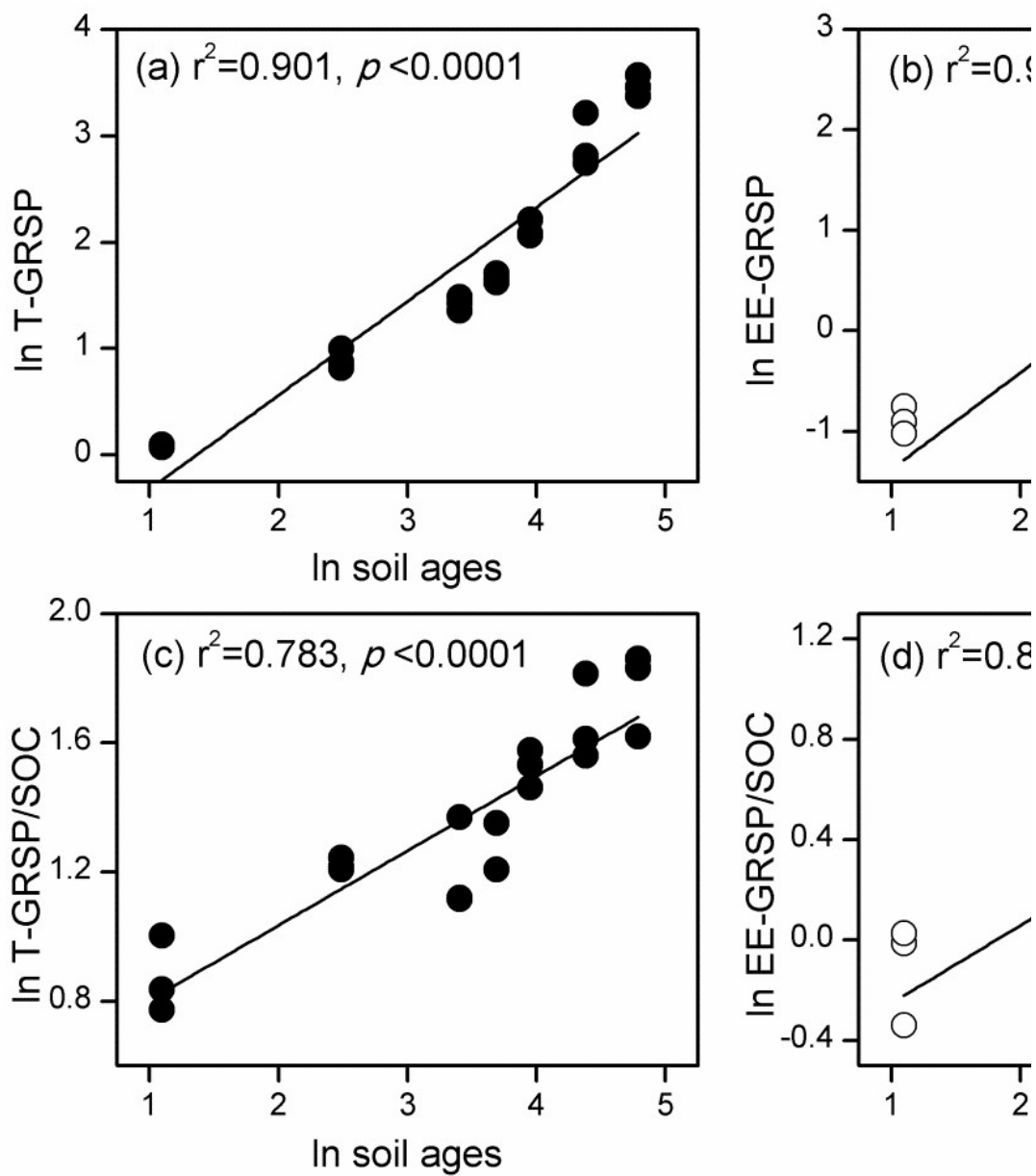


Figure 2

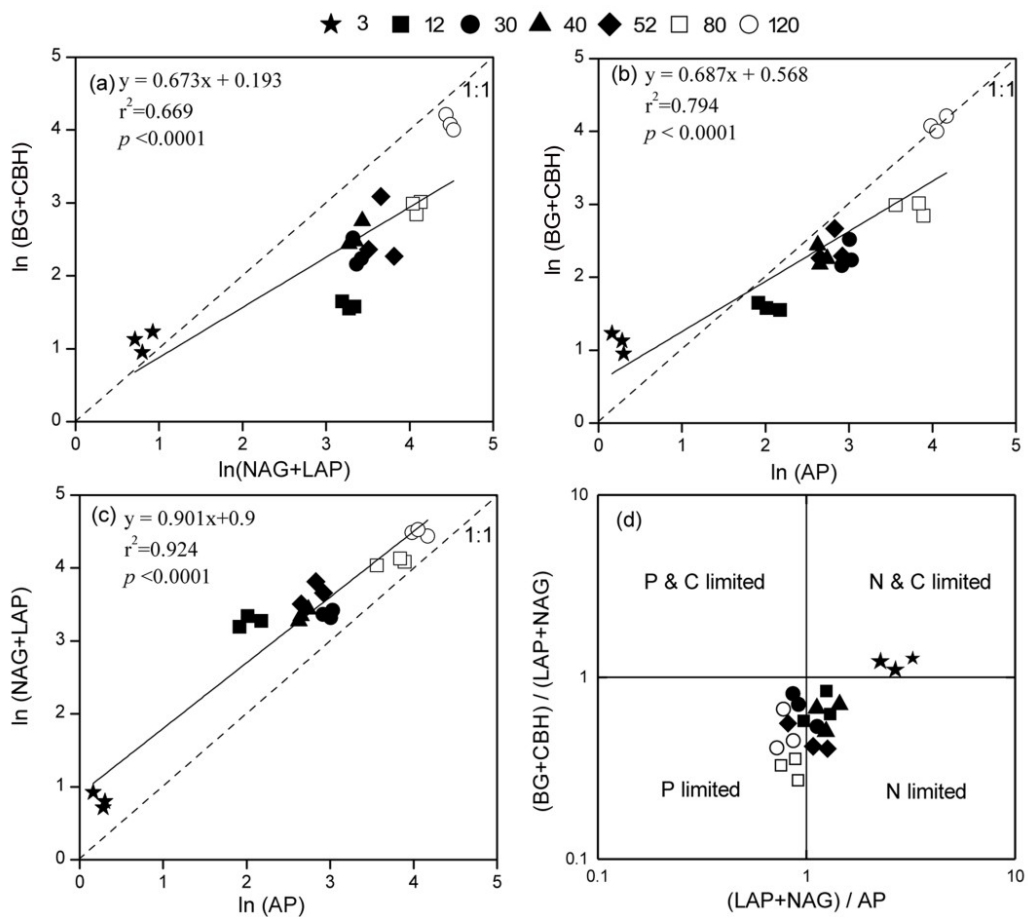


Figure 3

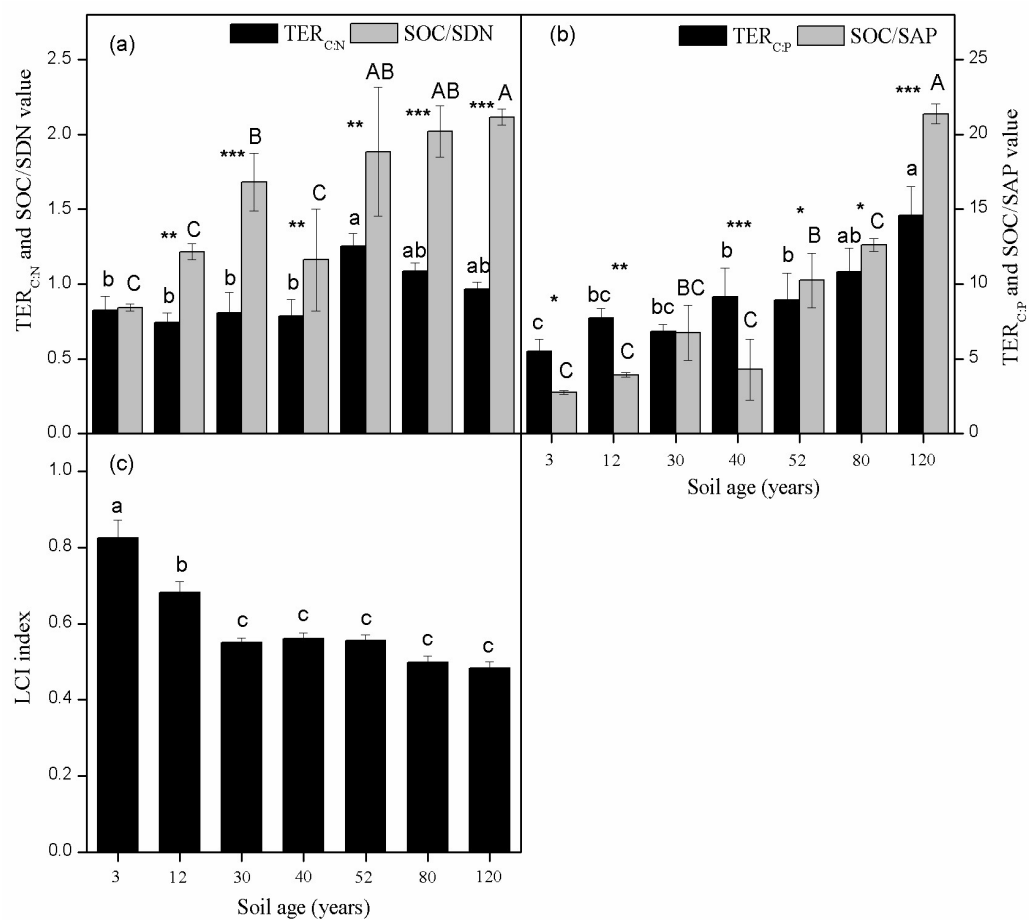


Figure 4

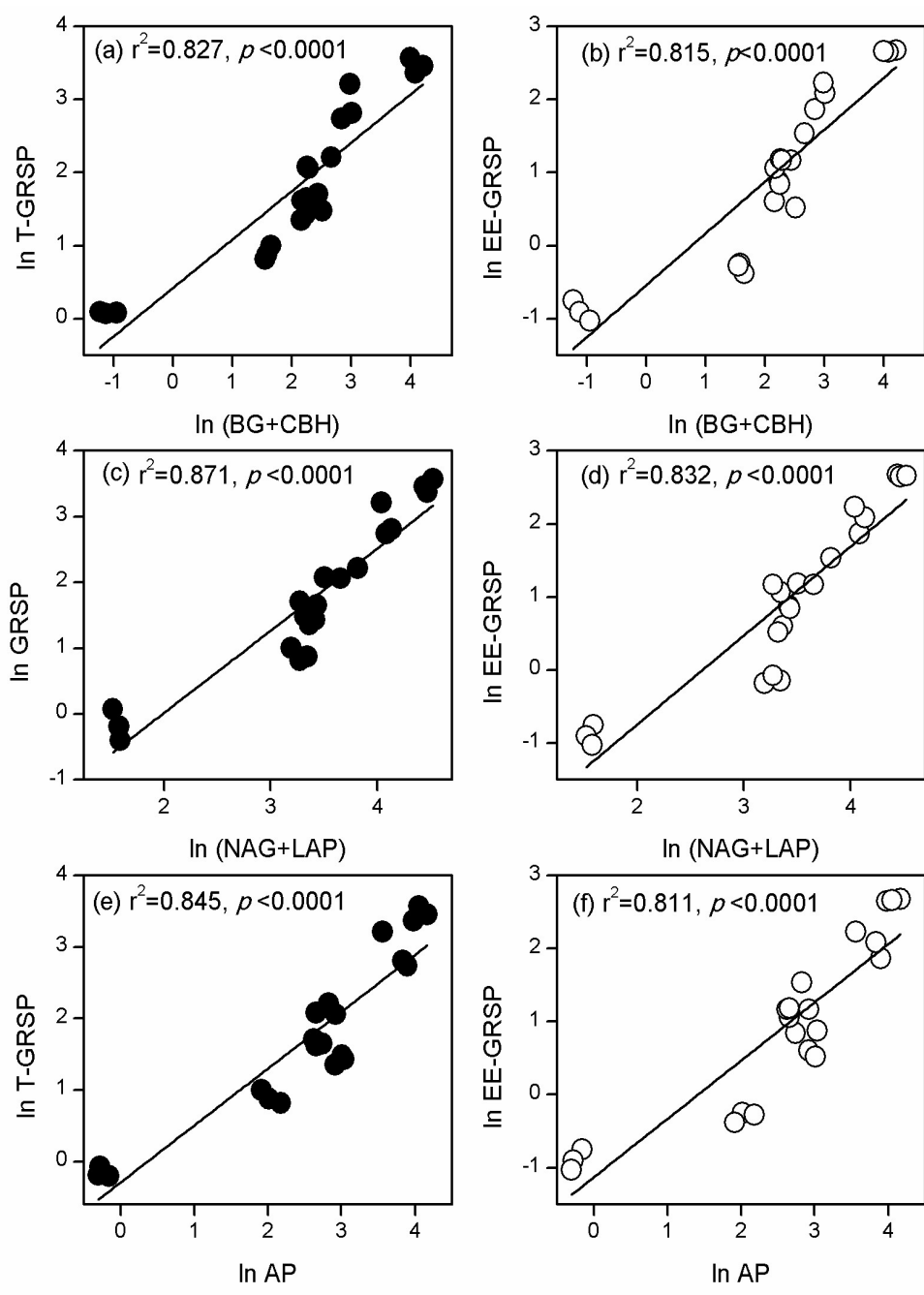


Figure 5

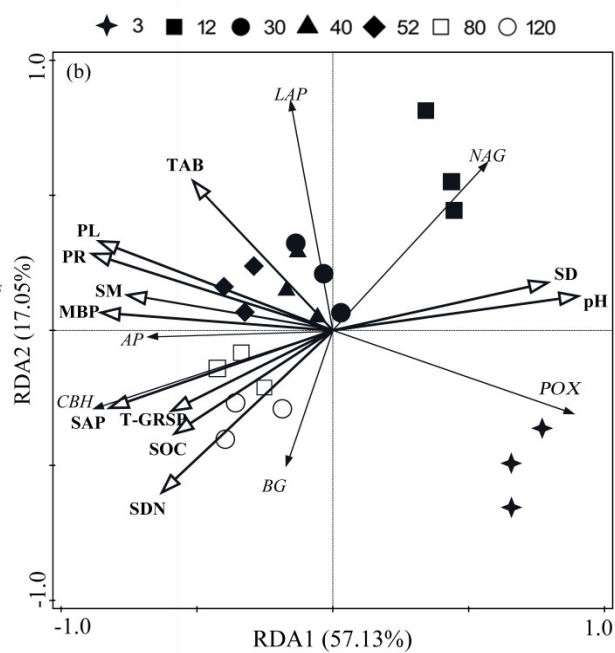
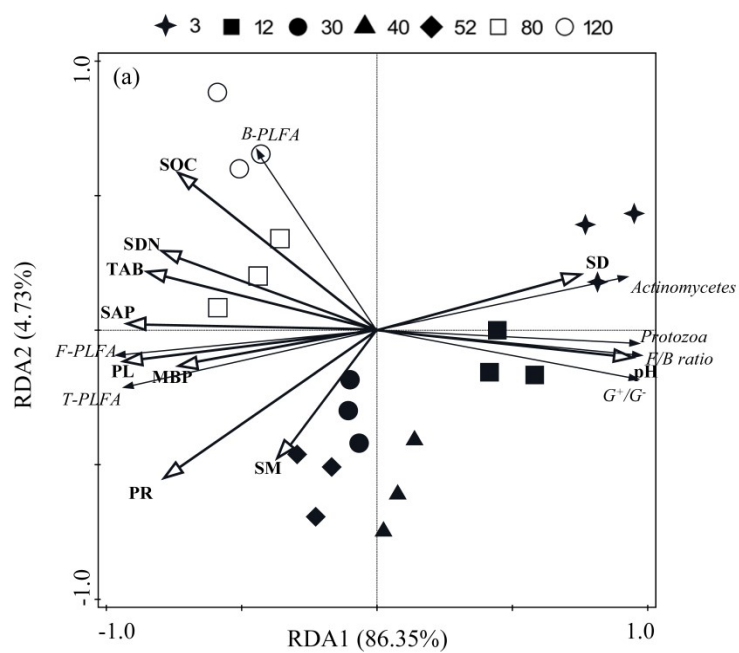
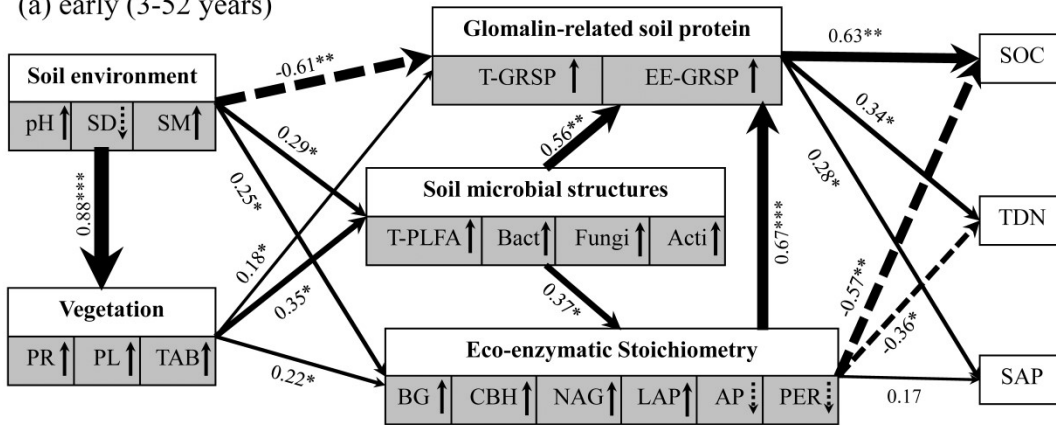


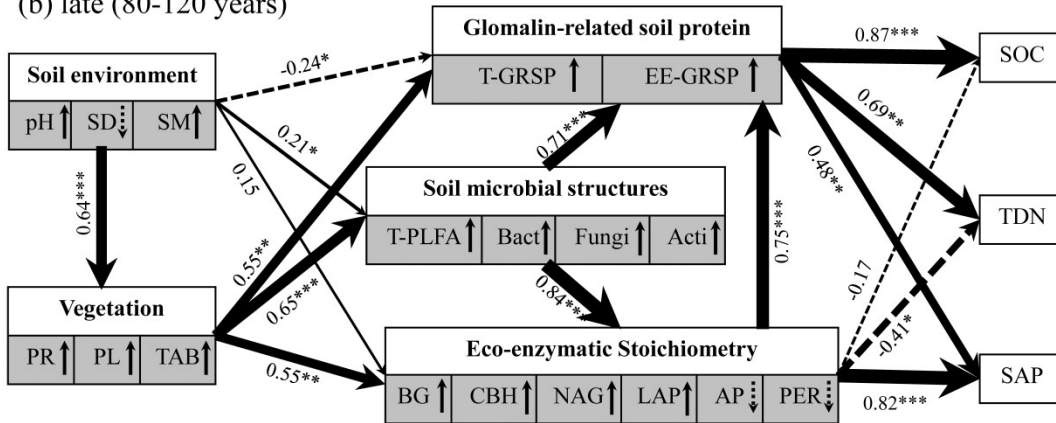
Figure 6

(a) early (3-52 years)



$\chi^2=3.252$, $df=13$, $P=0.112$, $AIC=85.01$, $GFI=0.973$, $RMSEA=0.013$

(b) late (80-120 years)



$\chi^2=2.752$, $df=13$, $P=0.167$, $AIC=95.43$, $GFI=0.915$, $RMSEA=0.023$

Figure 7